Proceedings of the European Conference Physics of Magnetism, Poznań 2014

# Electronic Band Structure of $Ru_3Sn_7$

M. Sahakyan* and V.H. Tran
Institute for Low Temperature and Structure Research, Polish Academy of Sciences,
Okólna 2, 50-422 Wrocław, Poland

The first-principle band structure calculations for $Ru_3Sn_7$ and $Mo_3Sb_7$ were carried out using the full-potential linearized muffin tin orbital method. It was shown that the valence band contribution is mainly due to the $4d$ electrons of Ru(Mo), while the contribution from the $5p$-Sn(Sb) orbitals is relatively small. Furthermore, the $4d$ and $5p$ orbitals located near the Fermi level have the non-hybridized characters, thus presumably contributing independently to the total density of states. A comparison of the density of states of two compounds reveals an essential difference in the structures and magnitudes. We estimated the mass enhancement factor and Stoner product and discussed these differences regarding to electronic and magnetic behaviour of these compounds.

DOI: 10.12693/APhysPolA.127.303
PACS: 71.15.Ap, 31.15.A–, 74.20.Pq

## 1. Introduction

Intermetallic $Ru_3Sn_7$ and $Mo_3Sb_7$, crystallizing in the cubic $Ir_3Ge_7$-type structure (space group $Im\bar{3}m$) amongst 20 another $T_3X_7$-type compounds (T is a transition metal, X is $p$-electron metalloid, mainly In, Ge, Ga, Sn), were reported in the middle of the 20th century [1]. As previously reported, $Ru_3Sn_7$ and $Mo_3Sb_7$ differ from one another in physical properties. $Mo_3Sb_7$ was firstly determined as an ordinary BCS-type superconductor with $T_c = 2.1$ K [2], and its superconducting state may be described by two BCS-like gaps with $2\Delta_1 \approx 4.0\ k_BT_c$ and $2\Delta_2 \approx 2.5\ k_BT_c$ [3]. These suggestions are being strengthened by muon spin-rotation $\mu$SR studies in the superconducting state [4]. In view of the fact that the effective mass of charge carriers is strongly enhanced and the magnetic penetration depth is relatively large compared to those of typical BCS superconductors, one expects that $Mo_3Sb_7$ would be a candidate of the bridge between two classes of the multiple-transition superconductors: high-$T_c$ and heavy-fermion superconductors [4]. Several important facts emerge from different electronic band structure calculations for $Mo_3Sb_7$ [5–8]. To encourage the interpretation based on two-gapped model, the electronic density of states and Fermi surface data have shown that the $4d$- and $sp$-electrons forming two bands differ from one another by the Fermi velocities, and in consequence they contribute differently to density of state (DOS) at the Fermi level, $E_F$ [3, 9]. Another interesting result is the appearance of a largest peak of DOS located at around –0.035 eV below $E_F$, pointing to the existence of the Van Hove singularity.

In contrast to $Mo_3Sb_7$, $Ru_3Sn_7$ appears to be diamagnetic at room temperature and becomes paramagnetic upon decreasing temperature below 170 K [10]. This behaviour together with a nonlinear temperature dependence of the resistivity at high temperatures has been ascribed to the role of the Ru $d$ orbitals at the Fermi level. We measured specific heat and electrical resistivity [5], as well as muon spin relaxation and inelastic neutron scattering [11] for $Ru_3Sn_7$. The obtained data were treated as a phonon reference for superconducting $Mo_3Sb_7$. In this work, we present the electronic band structure and density of states of $Ru_3Sn_7$ and $Mo_3Sb_7$, which were obtained using the full potential linearized muffin-tin orbital (FP-LMTO) method. Similarities and differences between DOS of these compounds will be discussed in terms of their electronic and magnetic behaviour. Previously, a large number of theoretical investigations were dedicated to $Mo_3Sb_7$ [5–8], while study on $Ru_3Sn_7$ was reported only by Häussermann et al. [7], who obtained from ab initio linear muffin-tin orbital method in the atomic sphere approximation (ASA) calculations.

## 2. Details of the calculations

The present data for $Ru_3Sn_7$ and $Mo_3Sb_7$ were obtained using FP-LMTO method augmented by a plane wave basis [12, 13]. The exchange-correlation energy was derived in the local density approximation. The self-consistent calculation of the electron charge density (after initial cycle of interactions) was performed using the 1728 $k$-points in the irreducible wedge of the Brillouin zone employing the tetrahedron method with the (12,12,12) $k$-mesh of the Brillouin zone. The exchange correlation potential was taken into account in the form of the Perdew and Wang [14, 15] and assuming generalized gradient approximation according to that given in [16]. The accuracies of matching of the spherical Hankel functions in real and reciprocal space were chosen to be 0.02 and 0.04. The number of divisions between nearest neighbors in the unit cell for the fast Fourier transform was 16. For the crystal structure, we used the experimental lattice parameter and atomic positions previously reported [5, 10], i.e., $a = 0.974$ nm; Ru at 12e (0.34514,0,0), Sn1 at 12d (0.25,0.0,0.5) and Sn2 at 16f-2 (0.1612, 0.1612, 0.1612). After structural optimization the atomic sphere radii of the Ru, Sn1 and Sn2 atoms are self-consistently found as follows $r_{Ru} = 2.527$ a.u.,

*corresponding author; e-mail: m.sahakyan@int.pan.wroc.pl

$r_{Sn1}$ = 2.65 a.u. and $r_{Sn2}$ = 2.63 a.u. The crystallographic data set for $Mo_3Sb_7$ was taken as in Ref. [3].

### 3. Results and discussion

In upper part of Fig. 1 we present the energy dependence of electronic density of states *N(E)* for $Ru_3Sn_7$ and corresponding energy band structure in the bottom part. The band structures have been calculated along the high symmetry directions in the bcc crystal, i.e., along [100], [110], and [111]. It turns out that the *N(E)* of $Ru_3Sn_7$ from our calculations is fully comparable to previously reported results [7]. Below $E_F$ there is a rich structure but one recognizes two main regions, one spans just below $E_F$ down to –0.3 Ry, and the second region is located around –0.55 Ry, relative to $E_F$. In the lowest energy range, the electronic states come mostly from the Sn *s* orbital, whereas in the higher energy regime *N(E)* consist of the contributions of both Sn *p* and Ru *d* derived bands. Here, the Ru *d* partial DOS is assertive. Above $E_F$, the contribution of the Ru *d* orbitals fades and the Sn *sp*- character becomes dominant. Instead of an energy gap as in $Mo_3Sb_7$ (see Fig. 2) we observe a deep minimum placed at 0.08 Ry.

In Fig. 2 we compare the DOS of $Mo_3Sb_7$ and $Ru_3Sn_7$ around the Fermi energy. It is notable that our results for $Mo_3Sb_7$ are in agreement with those obtained by the FPLO code [3] but a little different to those by the Korringa–Kohn–Rostoker (KKR) multiple scattering method [8]. In the *N(E)* from both the FP-LMTO and FPLO methods, the Fermi level is situated near the bottom, barring on the rise side of the local valley, on the contrary, the Fermi level obtained by the KKR method locates exactly at the top of the local maximum. Another difference is the contribution of the Sb 5*p* orbitals to the total DOS. While the KKR calculations have yielded equal inputs from Sb1 and Sb2 orbitals, our calculations have predicted, however, that the contribution of Sb1 *p*-orbitals is a factor of twice larger than that of Sb2. The observed differences could be related to the different initial input parameters in both methods. The DOS of $Ru_3Sn_7$ (right part of Fig. 2) and $Mo_3Sb_7$ have common features such as the 4*d* and 5*p* orbitals are located near the Fermi level and have a non-hybridized character. However, the *N(E)* of the considered compounds clearly differ in peak structures and magnitudes. For $Ru_3Sn_7$ the largest peak in the total electronic DOS is located at the energy of $\approx -0.0169$ Ry (–0.23 eV) relative to $E_F$, i.e., much lower than that in $Mo_3Sb_7$ ($\approx -0.0052$ Ry below $E_F$). This finding indicates that in the *N(E)* of $Ru_3Sn_7$ there exists no so-called Van Hove peak, and thus may suggest that the superconductivity in $Mo_3Sb_7$ would be associated with the Van Hove singularity. It is worthwhile to note that the sign of the slope of $N(E_F)$ is different in $Ru_3Sn_7$ and $Mo_3Sb_7$. Since the $E_F$ of $Ru_3Sn_7$ lies on a dip of *N(E)*, the derivative $dN(E_F)/dE$ should be negative in contrast to the situation in $Mo_3Sb_7$, where $dN(E_F)/dE$ is presumably positive. This hints that the signs of thermoelectric power of these compounds will

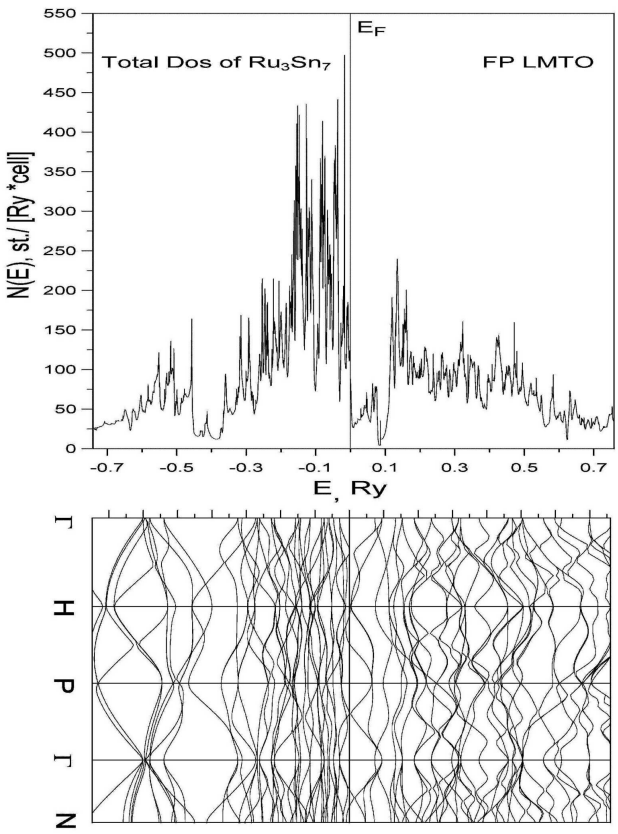


Fig. 1. Density of states and band structure of $Ru_3Sn_7$.

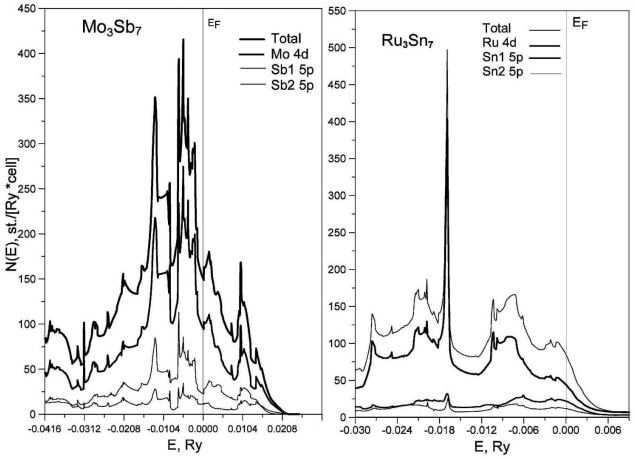


Fig. 2. DOS of $Mo_3Sb_7$ (left part) and $Ru_3Sn_7$ (right part). The total DOS and partial densities of the Mo, Sb1 Sb2 and Ru, Sn1 and Sn2 are shown respectively in the top, middle and bottom of each part.

be opposed, if they have the same type of charge carriers. Otherwise, at the $E_F$, the Ru *d*-orbital contribution to the total DOS is roughly 54%, compared to 67% in the case of Mo *d*-orbital. The electronic DOS of $Ru_3Sn_7$ at $E_F$ is 86 st./[Ry cell] = 14.3 st./[Ry atom], and its considerably reduced as compared to that in $Mo_3Sb_7$ ($\approx$ 150 st./[Ry cell] = 25 st./[Ry atom]).

This corresponds to a bare Sommerfeld ratio $\gamma_{\rm bare}$ = 14.9 mJ $\rm mol^{-1}_{Ru_3Sn_7}K^{-2}$ and 25.9 mJ $\rm mol^{-1}_{Mo_3Sb_7}K^{-2}$, respectively. These values are noticeably smaller than the experimental values of $\gamma_{\rm exp}$ = 19.5 mJ $\rm mol^{-1}_{Ru_3Sn_7}K^{-2}$ [5] and 34.5 mJ $\rm mol^{-1}_{Mo_3Sb_7}K^{-2}$ [3]. As discussed previously [3], a high $\gamma_{\rm exp}$ value of $Mo_3Sb_7$ could be due to mass enhancement coupling, expressed by a factor $\lambda_\gamma \approx 0.64$. A comparison of $\gamma_{\rm bare}$ and $\gamma_{\rm exp}$ for $Ru_3Sn_7$ confesses the factor $\lambda_\gamma$ of this compound to take a value of 0.308.

The weak magnetism of $Ru_3Sn_7$ and $Mo_3Sb_7$ seems to be understood if estimating the Stoner product $S = N(E_{\rm F})I$, where $I$ is the Stoner integral. Using the value $I$ = 0.022 Ry for Ru and Mo [17], we deduced $S$ = 0.31 and 0.55 for $Ru_3Sn_7$ and $Mo_3Sb_7$, respectively. Apparently, the $S$ factor of the studied compounds does not meet the Stoner criterion for the occurrence of itinerant ferromagnetism ($> 1$) and collaborates their nonmagnetic ground state. A smaller $S$ value in $Ru_3Sn_7$ compared to $Mo_3Sb_7$ reveals reasonably why the magnetic interactions in $Ru_3Sn_7$ are weak and more stronger in $Mo_3Sb_7$.

In Fig. 3 we show the calculated Fermi surface for $Ru_3Sn_7$. The unique unit cell center is chosen as (0.5,0.5,0.5) with a cube division grid (10,10,10). Every $k$-point is computed as the cube point minus the origin vector.

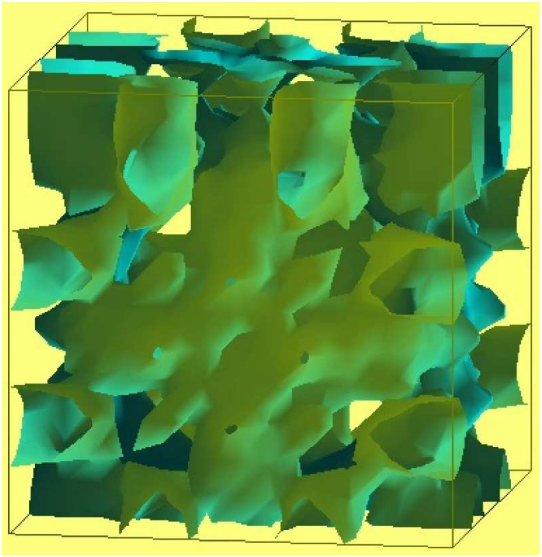

Fig. 3. Fermi surface of $Ru_3Sn_7$.

As one expects, the topology of the Fermi surface of $Ru_3Sn_7$ is much different from that of $Mo_3Sb_7$ [9], for which nesting is involved. Therefore, if superconductivity is associated with the FS nesting, this is obviously absent in $Ru_3Sn_7$.

## 4. Summary

By means of the FP-LMTO method, we have calculated the electronic density of states of $Ru_3Sn_7$ and superconducting $Mo_3Sb_7$. The DOS of two compounds have common features such as the $4d$ and $5p$ orbitals are located near the Fermi level and have a non-hybridized character. However, there exists clear distinction in the structures and magnitudes of the DOS. The $E_{\rm F}$ of $Ru_3Sn_7$ lies in a dip of $N(E)$ and far away from the highest DOS, while that of $Mo_3Sb_7$ locates just above the highest DOS and at the rise side of a local valley. For $Ru_3Sn_7$ we found $N(E_{\rm F})$ = 86 st./Ry cell, corresponding to the mass enhancement factor of $\lambda_\gamma$ = 0.308 and the Stoner product $S$ = 0.31, compared to $N(E_{\rm F})$ = 150 st./Ry cell, $\lambda_\gamma$ = 0.64 and the Stoner product $S$ = 0.55 in the case of $Mo_3Sb_7$. In conclusions, the observed differences between the two considered compounds in the DOS and FS may explain their different electronic and magnetic behaviour.

## Acknowledgments

Financial support from the project 2011/01/B/ST3/04553 of the National Science Centre of Poland.

## References

[1] F. Hulliger, *Nature* **209**, 500 (1966).

[2] Z. Bukowski, D. Badurski, J. Stępień-Damm, R. Troć, *Solid State Commun.* **123**, 283 (2002).

[3] V.H. Tran, W. Miiller, Z. Bukowski, *Acta Mater.* **56**, 5694 (2008).

[4] V.H. Tran, A.D. Hillier, D.T. Adroja, Z. Bukowski, *Phys. Rev. B* **78**, 172505 (2008).

[5] V.H. Tran, W. Miiller, *Acta Phys. Pol. A* **115**, 83 (2009).

[6] E. Dashjav, A. Szczepenowska, H. Kleinke, *J. Mater. Chem.* **12**, 345 (2002).

[7] U. Häussermann, M. Elding-Pontén, Ch. Svensson, S. Lidin, *Chem. Eur. J.* **4**, 1007 (1998).

[8] B. Wiendlocha, J. Tobola, M. Sternik, S. Kaprzyk, K. Parlinski, A.M. Oleś, *Phys. Rev. B* **78**, 060507 (2008).

[9] V.H. Tran, W. Miiller, Z. Bukowski, *Phys. Rev. Lett.* **100**, 137004 (2008).

[10] B.C. Chakoumakos, D. Mandrus, *J. Alloys Comp.* **281**, 157 (1998).

[11] V.H. Tran, A.D. Hillier, D.T. Adroja, Z. Bukowski, W. Miiller, *J. Phys. Condens. Matter* **21**, 485701 (2009).

[12] S.Y. Savrasov, D.Y. Savrasov, *Phys. Rev. B* **46**, 12181 (1992).

[13] S.Y. Savrasov, *Phys. Rev. B* **54**, 16470 (1996).

[14] J.P. Perdew, Y. Wang, *Phys. Rev. B* **33**, 8800 (1986).

[15] J.P. Perdew, Y. Wang, *Phys. Rev. B* **45**, 13244 (1992).

[16] J.P. Perdew, K. Burke, Y. Wang, *Phys. Rev. B* **54**, 16533 (1996).

[17] J.F. Janak, *Phys. Rev. B* **16**, 255 (1977).